Aging and Sex Shape the Intrinsic and Synaptic Properties of Mitral Cells in the Mouse Olfactory Bulb

Dan Zhao , Meigeng Hu , Cameron Paige Vicknair , Yaping Li , Shaolin Liu *

Posted Date: 5 March 2026

doi: 10.20944/preprints202603.0474.v1

Keywords: aging; sex-dependent; mitral cells; olfactory behavior; intrinsic excitability; synaptic transmission

 doi:10.20944/preprints202603.0474.v1

Article

Aging and Sex Shape the Intrinsic and Synaptic Properties of Mitral Cells in the Mouse Olfactory Bulb

Dan Zhao, Meigeng Hu, Cameron Paige Vicknair, Yaping Li and Shaolin Liu *

Center for Neurological Disease Research, Department of Physiology and Pharmacology, Department of Biomedical Sciences, University of Georgia College of Veterinary Medicine, 501 D.W. Brooks Drive, Athens, GA 30602

* Correspondence: shaolin.liu@uga.edu

Highlights

What are the main findings?

- Aging and sex jointly modulate olfactory-guided behavior, revealing sex-dependent vulnerability in late-life olfactory function.
- Mitral cell intrinsic excitability is coordinatedly remodeled in an age- and sex-dependent manner across the lifespan.
- Excitatory synaptic drive onto mitral cells declines with age in both sexes, indicating weakened afferent input in advanced age.

What is the implication of the main finding?

- Mitral cells represent a critical cellular intersection where aging and sex converge to shape olfactory circuit vulnerability and may serve as biomarkers for neurodegenerative risk.

Abstract

Aging is accompanied by a progressive decline in olfactory function, which affects a large proportion of older adults and has substantial consequences for nutrition, safety, and overall quality of life. Increasing evidence indicates that sex-dependent differences in ol-factory processing become more pronounced with advancing age, particularly in late life. However, the cellular basis beyond the peripheral level by which aging and sex interact to influence neuronal and synaptic functions in central structures remains poorly under-stood. To bridge this gap, we compared behavioral outcomes, intrinsic and synaptic properties of the olfactory bulb (OB) output neurons mitral cells (MCs) that receive direct sensory input from odor receptor neurons and integrate olfactory information to most higher order brain regions, in male and female C57BL/6J mice of three ages spanning the natural lifespan. Consistent with human studies and the key role of mitral cells in trans-forming input to output in the OB, our behavioral tests showed that both aging and sex significantly influenced odor detection performance, which declined with age, particular-ly in females while locomotor activity remained preserved. At the cellular level, our whole-cell patch-clamp recordings in OB slices demonstrated that MCs in male mice across the lifespan exhibit a gradual decline in excitability and synaptic strength with age, while female mice maintain stable function until advanced age, when marked alterations emerge. This study provides the first physiological evidence of the joint influence of aging and sex on the functional operation of the OB at the cellular and synaptic levels. Consid-ering olfactory impairment as the earliest and most sensitive indicator of the age-dependent and sex-biased neurodegenerative disorders such as Alzheimer's disease and Parkinson's disease, our findings provide functional insights not only into normal aging-induced

 doi:10.20944/preprints202603.0474.v1

olfactory deficits but also into the future development of early biomarkers and intervention strategies for these neurodegenerative disorders.

Keywords: aging; sex-dependent; mitral cells; olfactory behavior; intrinsic excitability; synaptic transmission

1. Introduction

Aging is a fundamental biological process that reshapes sensory perception and neural function across the lifespan(Kondo et al., 2020). Among the sensory modalities, olfaction is especially vulnerable to age-related decline and is often experienced as an invisible impairment, as it develops gradually and frequently goes unrecognized by affected individuals(Olofsson et al., 2020). Population studies consistently show that olfactory dysfunction becomes highly prevalent in late life, affecting a substantial proportion of adults aged 65–80 and increasing further beyond this age(Doty and Kamath, 2014). Unlike visual or auditory deficits, olfactory loss lacks widely effective corrective technologies, rendering its functional consequences difficult to compensate(Tzeng et al., 2021). As a result, age-related olfactory decline is associated with impaired nutrition, reduced safety awareness, diminished quality of life, and increased mortality risk(Attems et al., 2015, Boesveldt et al., 2017, Croy et al., 2014).

Compared with the robust effects of aging, sex-related influences on olfactory decline are more complex and exhibit clear functional specificity in later life(Tzeng et al., 2021). Although women generally outperform men on olfactory measures during much of adulthood, this advantage does not translate into identical aging trajectories in the two sexes(Sorokowski et al., 2019). Instead, sex differences become more pronounced in older age and depend strongly on the olfactory domain being assessed. In older adults, basic odor sensitivity declines largely as a function of age, with relatively modest and inconsistent sex differences. By contrast, more pronounced sex effects emerge in higher-order olfactory functions that rely on central information integration, particularly odor identification, where older men tend to exhibit greater functional impairment(Xu et al., 2020, Yang and Pinto, 2016). Importantly, this male disadvantage at the level of behavioral performance coexists with evidence that aging women exhibit earlier or more pronounced vulnerability in central neural substrates supporting olfactory processing, including greater volumetric reduction in limbic and associative regions and increased risk for neurodegenerative disease(Alotaibi et al., 2023, Beam et al., 2018, Zhu et al., 2021). This shared vulnerability underscores the importance of distinguishing age-driven from sex-dependent sources of olfactory decline and highlights the need to understand how aging and sex jointly shape the integrity of olfactory circuits.

Central to olfactory processing is the olfactory bulb (OB), the primary site for integrating odor signals directly received from olfactory sensory neurons(Nagayama et al., 2014). The OB contains complex neural circuits composed mainly of excitatory projection neurons, such as mitral and tufted cells(Kensaku, 2014, Starr et al., 2025, Vinograd et al., 2019), and diverse inhibitory interneurons, particularly granule and periglomerular cells(Arruda et al., 2013). Unlike inhibitory interneurons, which continuously regenerate through adult neurogenesis and significantly enhance olfactory plasticity(Yamaguchi, 2014, Dejou et al., 2024), mitral and tufted cells are generated early during development and persist throughout life without renewal(Díaz-Guerra et al., 2013, Hirata, 2024). Consequently, these excitatory neurons are especially prone to cumulative functional decline associated with aging and sex-specific differences. Particularly, mitral cells (MCs) serve as the primary OB output neurons and convey processed olfactory information to higher cortical areas critical for odor perception and memory(Mori and Sakano, 2021). Given their longevity and susceptibility to progressive damage, MCs provide an ideal model for exploring how aging and biological sex impact neuronal function, connectivity, and sensory processing. Understanding these interactions could clarify the mechanisms behind age-associated olfactory impairment and its relationship with neurodegenerative disease pathology.

 doi:10.20944/preprints202603.0474.v1

Although MCs are essential to olfactory circuit function, the cellular mechanisms by which aging and biological sex shape their excitability and synaptic integration remain incompletely understood. We found that aging and biological sex influence olfactory function, with older animals showing reduced efficiency in odor-guided foraging and this impairment being most pronounced in females, while locomotor activity remained intact. These behavioral differences were accompanied by marked alterations in mitral cell physiology, prompting us to systematically examine intrinsic membrane properties, action potential dynamics, firing patterns, and excitatory synaptic transmission across the lifespan using whole-cell patch-clamp recordings in both sexes. Our results demonstrate that MC physiology undergoes complex, age- and sex-dependent remodeling: intrinsic excitability increases with age in males, but peaks at midlife and then declines in females, while action potential and membrane properties follow distinct aging trajectories in each sex. At the synaptic level, we observed a progressive decline in excitatory synaptic input to MCs in both sexes with advancing age, regardless of underlying membrane property changes. This reduction in synaptic drive likely limits the functional output of OB circuits and may contribute to the increased risk of olfactory dysfunction and neurodegenerative disease in the elderly. Together, these findings provide a cellular and mechanistic framework for understanding how physiological aging and sex interact to influence sensory processing and disease vulnerability in the olfactory system.

2. Materials and Methods

2.1. Animals

Wild-type C57BL/6J mice of both sexes were originally obtained from The Jackson Laboratory (Bar Harbor, ME, USA) and subsequently bred in-house to generate experimental cohorts. For behavioral assessments, mice were assigned to two age categories: adult (17–21 weeks old) and aged (85–123 weeks old). The open-field test was performed using adult (males, n = 15; females, n = 16) and aged mice (males, n = 10; females, n = 16). For the buried food and visible food assays, the same age ranges were examined; these tests were conducted using all animals from the open-field cohort with additional animals included to increase sample size, resulting in larger group numbers (adult: males, n = 20; females, n = 18; aged: males, n = 14; females, n = 15). For electrophysiological recordings, an independent cohort was organized into three physiologically defined age groups based on established aging criteria: young adults (19 weeks old; 3 males, 3 females), middle-aged adults (37 weeks old; 3 males, 4 females), and aged mice (123 weeks old; 4 males, 3 females), representing distinct stages from mature adulthood through advanced senescence(Flurkey et al., 2007). This design enables systematic assessment of age-dependent changes in mitral cell electrophysiological properties across the lifespan. All mice were maintained under specific pathogen-free conditions on a 12-h light/dark cycle with ad libitum access to food and water. Animals were monitored daily by our animal resource and care team to ensure their overall health and suitability for behavioral and electrophysiological experiments. All procedures adhered to the National Institutes of Health (NIH) guidelines for the care and use of laboratory animals and were approved by the Institutional Animal Care and Use Committee of the University of Georgia.

2.2. Behavioral tests

2.2.1. Open field test

To evaluate spontaneous locomotor activity and exploratory behavior, mice were tested in a standard open-field paradigm(Seibenhener and Wooten, 2015). The open-field arena consisted of a square, opaque white acrylic box (45 × 45 × 45 cm). At the start of each trial, the mouse was gently placed in the center of the arena and allowed to freely explore for 15 min under consistent lighting conditions. All movements were recorded using a top-mounted camera connected with the ANY-maze Video Tracking System (version 7.51, Stoelting Co.). The quantitative parameter of total

 doi:10.20944/preprints202603.0474.v1

distance traveled was extracted to assess overall activity levels and responses to the novel environment.

2.2.2. Buried food and visible food test

Odor detection was assessed using a buried food test(Machado et al., 2018), which is based on the odor-driven foraging behavior. Briefly, animals were food-restricted for 24 hours with free access to water before the test to increase their motivation for food search. To start the trial, each mouse was placed in a clean cage filled with 1-inch-thick fresh bedding, at the bottom of which a single chow pellet was hidden at a fixed location so that the animal needed to search and locate the invisible food based on its olfaction. The mouse was released on the opposite side of the buried food to initiate exploration. The latency to uncover and begin eating the buried pellet was recorded as a measure of successful olfactory performance. Same procedures were used for the visible food test, except that the food pellet was placed on the top surface of the bedding material to enable visual-guided search.

2.3. Slice Preparation

Acute OB slices were prepared from mice after deep anesthesia with isoflurane using the IACUC-approved open-drop method prior to decapitation. Briefly, coronal slices (350 μm) were cut with a VT1200s vibratome (Nussloch, Germany) in an ice-cold and oxygenated (95% O_2–5% CO_2) NMDG-based artificial Cerebrospinal Fluid (NMDG-aCSF) containing (in mM) 90 NMDG, 2.5 KCl, 1.2 NaH_2PO_4, 30 $NaHCO_3$, 25 glucose, 20 NaHEPES, 5 Sodium ascorbate, 2 Thiourea, 3 Sodium pyruvate, 10 $MgSO_4$, 0.5 $CaCl_2$ (pH 7.40, 300 mOsm). After 30 min of incubation in NMDG aCSF at 30°C, slices were then transferred to HEPES-based aCSF at room temperature until they were used for recordings. HEPES-based aCSF was continuously bubbled with 95% O_2–5% CO_2 and had the composition (in mM): 92 NaCl, 2.5 KCl, 1.2 NaH_2PO_4, 30 $NaHCO_3$, 25 glucose, 20 NaHEPES, 2 Sodium ascorbate, 2 Thiourea, 3 Sodium pyruvate, 2 $MgSO_4$, 2 $CaCl_2$ (pH 7.40, 300 mOsm). During the experiments, slices were perfused at 150 mL h^{-1} with recording aCSF. Recording aCSF was equilibrated with 95% O_2–5% CO_2 and warmed to 30°C and had the composition (in mM): 125 NaCl, 2.5 KCl, 1.25 NaH_2PO_4, 25 $NaHCO_3$, 10 glucose, 2 $MgSO_4$, 2 $CaCl_2$ (pH 7.40, 300 mOsm).

2.4. Electrophysiology

Whole cell patch clamp recordings were made from MCs in OB slices visualized using Eclipse FN1 (Nikon, Japan) fixed-stage upright microscope with near-infrared differential interference contrast (DIC) optics. MCs were preselected for recording based on their soma location and dendrite projections. Neuron type identities were subsequently verified by electrophysiological properties and post hoc morphology reconstruction.

To visualize the recorded neurons and their dendrites followed by reconstruction, biocytin (0.2%) was included in the internal solution. Signals in current or voltage clamp were recorded with an Integrated Patch Amplifier (IPA, Sutter Instrument) and SutterPatch® Data Acquisition Software SutterPatch 3.1. Using the IPA's built-in filter, data were sampled at 10 kHz and filtered at 10 kHz. The software's automated compensation feature was used to apply series resistance compensation and electrode compensation automatically. Data analysis was performed using the same software (SutterPatch 3.1). Recording electrodes (5-7 MΩ) were pulled from thin-wall glass capillary tubes with filament (Sutter Instrument, Novato, CA, USA). Electrode solution contained (in mM) 4 EGTA, 12 KOH, 0.5 $CaCl_2$, 117 K-gluconate, 10 KCl, 10 HEPES, 3 Mg-ATP, 0.3 Na_2-GTP, and 7 Na_2-Phosphocreatine (pH 7.26, 290 mOsm).

2.5. Immunohistochemical Staining

Brain slices with biocytin (0.2%, w/v)-filled neurons were transferred to 4% paraformaldehyde (PFA) immediately after recording and kept at RT for 30 min. Slices were washed three times (3 min each) with 0.05 M phosphate-buffered saline (PBS) before being incubated in a blocker solution on a

 doi:10.20944/preprints202603.0474.v1

shaker for 1 h. Blocker solution contains 10% (v/v) normal donkey serum, 2% (v/v) Bovine Serum Albumin, 0.25% Triton X-100 in 0.05 M PBS. Then the blocker solution was replaced by a fresh blocker solution containing streptavidin-CY3 (1.8 μg/ml) and the reaction container was covered with aluminum foil to prevent light exposure at room temperature on a shaker for 5 h. To terminate streptavidin-CY3 staining, slices were rinsed with 0.05 M PBS for three times (5 min each) before being treated with 0.05 M PBS containing 40,6-diamidino-2-phenylindole (DAPI; 50 μg/ml) to stain cell nuclei at room temperature in the dark for 10 min. After three times of wash (5 min each) with PBS to terminate DAPI staining, slices were wet mounted and cover-slipped with Vectashield media. Cells were scanned and reconstructed under a confocal microscope.

2.6. Data Analysis

Behavioral data were analyzed using the ANY-maze Video Tracking Software (version 7.51, Stoelting Co.). Results are presented as mean ± standard error of the mean (SEM). To quantify the effects of age and sex on behavior, a Two-Way ANOVA was performed with age and sex as between-subject factors in Origin 2025. Electrophysiological signals were analyzed using Igor Pro 9.05 software (WaveMetrics). Resting membrane potential (RMP) was recorded in current clamp without any current injection immediately following break into the whole-cell configuration. Membrane resistance (R_m) was calculated from the slope of the linear fit of the current–voltage relationship obtained during hyperpolarizing current injections. Action potential (AP) characteristics, including threshold, amplitude, 50% AP duration, afterhyperpolarization (AHP), and firing frequency, were measured under two distinct current-clamp conditions: spontaneous and evoked AP firing. Spontaneous APs were recorded without external current injection. Evoked APs were elicited by delivering a series of 500 ms current steps every 5 s, starting from 0 pA and increasing by 20 pA/step until reaching a maximum of 220 pA. For quantification, AP parameters in the spontaneous condition were calculated as the average of all spontaneous spikes, whereas for evoked APs, only the first spike elicited at threshold current was analyzed, as it most closely resembles the intrinsic excitability in response to depolarizing stimuli. Spike threshold was defined as the point at which membrane depolarization acceleration began. Spike amplitude was measured as the voltage difference between AP threshold and its peak value. The 50% AP duration was determined as the interval between the rising and falling phases of the spike at half-maximal amplitude. The AHP was quantified as the voltage difference between AP threshold and the most negative potential immediately following repolarization. AP frequencies were calculated by taking the reciprocal of inter-spike intervals, defined as the time interval between consecutive spikes. Spontaneous excitatory postsynaptic currents (EPSCs) were recorded in whole-cell voltage-clamp with a holding potential of −60 mV. A 3-minute trace was collected and analyzed for each cell. Events were detected using the event detection module built in the SutterPatch software with a template defined by a rise time of 5 ms and a decay time of 10 ms. Statistical comparisons between groups were conducted using Tow-Way ANOVA followed by Holm–Bonferroni correction or Two-Sample t-Test followed by Welch Correction, while the cumulative probability of sEPSC frequency or amplitude were compared with the Nonparametric Kolmogorov-Smirnov Test in Origin 2025.

3. Results

3.1. Age- and sex-dependent differences in olfactory behaviors

To investigate the impact of sex and age on locomotor activity, we examined male and female mice at two age stages, 17-21 weeks (adults) and 85-123 weeks (aged), via the open field test (Figure 1A). Overall, we observed a significant effect of age on locomotor activity ($F(1, 54) = 6.90$, $p = 0.01$) but no significant effect of sex ($F(1, 54) = 0.43$, $p = 0.52$) (Figure 1B). When assessing the effect of age within each sex, we found that only aged males exhibited a significant increase in total distance travelled compared to young adult males ($p = 0.01$). In contrast, no significant differences were observed between males and females within either age group. Interestingly, aged mice exhibited a

 doi:10.20944/preprints202603.0474.v1

greater total distance traveled in the open field than young adults. Although locomotor activity is generally reported to decline with age(Yanai and Endo, 2021), several studies have shown that aging can alter habituation processes and modify the organization of exploratory behavior across repeated exposures to a novel environment(Deacon et al., 2009, Smith and Hopp, 2023, Rosenthal et al., 1989). These findings suggest that the increased distance observed in aged males reflects age-related differences in exploratory engagement rather than improved motor function and confirm that locomotor capacity remained sufficient for subsequent olfactory testing.

Building on these observations, we next evaluated animal's ability to detect odors using the buried food test (Figure 1B). It took substantially more time for both aged males and females to identify and retrieve the hidden pellet compared to their respective adult groups, indicating robust age-associated impairments in odor detection ($F(1, 63) = 98.81$, $p < 0.0001$). A sex difference was observed in aged animals, with females exhibiting longer latencies than males ($p < 0.0001$), whereas adult animals showed no significant difference. To ensure that these prolonged latencies reflected olfactory deficits rather than non-olfactory factors, we conducted a visible food test with the pellet placed on the bed-ding surface (Figure 1C). Under this condition, latencies were comparable across groups, except that aged males exhibited longer latencies than aged females ($p < 0.05$).

Together, these findings demonstrate that both aging and sex significantly shape ol-factory function, with olfactory impairment emerging in late life and presenting more prominently in females. The intact performance across all groups in the visible food test confirms that these differences arise from olfactory processing rather than motivational or visual–motor limitations.

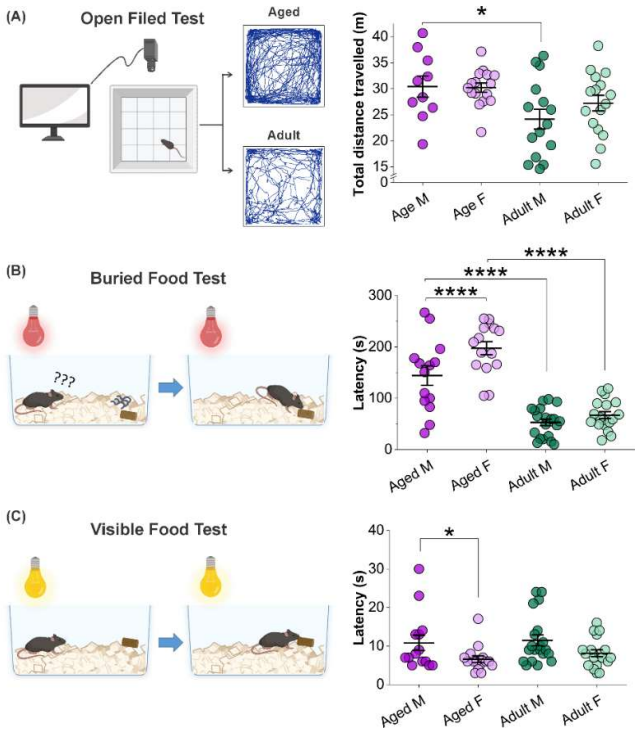

Figure 1. Age- and Sex-Dependent Differences in olfactory behaviors. (**A**) Representative locomotion tracings of aged and young adult mice in the open field test (left panel). Statistical graph showing the total distance traveled (right panel; aged: males n = 10, females n = 16; adult: males n = 15, females n = 16). (**B**) Schematic illustration of the buried food test (left panel). Latency to locate the buried pellet in aged and adult mice of both sexes (right panel; aged: males n = 14, females n = 15; adult: males n = 20, females n = 18). (**C**) Schematic illustration of the visible food test (left panel). Latency to retrieve the visible pellet in adult and aged mice of both sexes (right panel). Sample sizes match those of the buried food test). Each data point represents a parametric value from one animal. Statistical comparison and significance were conducted and determined by Two-way ANOVA with Holm–Bonferroni correction; *$p < 0.05$, ****$p < 0.0001$.

 doi:10.20944/preprints202603.0474.v1

3.2. Age- and sex-dependent age effects on mitral cell membrane properties

Whole-cell patch clamp recordings were performed under IR-DIC optics using pipettes containing biocytin, followed by post hoc biocytin immunostaining to confirm the characteristic morphology of mitral cells (MCs; Figure 2A).

Analyses of membrane properties revealed that age and sex interacted to shape mi-tral cell intrinsic physiology. Membrane resistance (R_m) was quantified across three age groups in male and female mice to assess age- and sex-related changes in intrinsic excita-bility. Two-Way ANOVA demonstrated a significant interaction between age and sex on Rm ($F(2, 84) = 3.99$, $p = 0.02$). In male mice, R_m increased progressively with age, showing a significant elevation at both 37- and 123-week groups compared to 19-week animals (both $p < 0.01$; Figure 2B). This increase in R_m suggests reduced membrane conductance, poten-tially enhancing MC sensitivity to synaptic input. In contrast, female mice showed no sig-nificant age-related differences in R_m across the three age groups. Notably, a sex difference was observed only in the aged group, in which males showed significantly greater Rm than females (123 weeks; $p < 0.0001$), suggesting greater excitability in aged males and pointing to an interaction between sex and age in regulating OB output.

The resting membrane potential (RMP) also varied as a joint function of age and sex, with a significant interaction detected by Two-Way ANOVA ($F(2, 79) = 3.56$, $p = 0.03$). In males, RMP was significantly more depolarized at 37 weeks than at 19- and 123-weeks ($p < 0.05$; Figure 2C), indicating increased excitability in the mid-age group of animals. Con-versely, female MCs exhibited a negative correlation between RMP and age, with a pro-gressive hyperpolarization from 19 to 123 weeks. A significant sex difference in the RMP was detected at both 37 and 123 weeks, with female MCs displaying more hyperpolarized values than males ($p < 0.05$), implying reduced excitability in females at this age.

Taken together, these findings demonstrate for the first time that aging and sex jointly influence Rm and RMP in mitral cells, highlighting an intricate interaction between these two factors in shaping output neuron excitability and potentially olfactory processing in the OB.

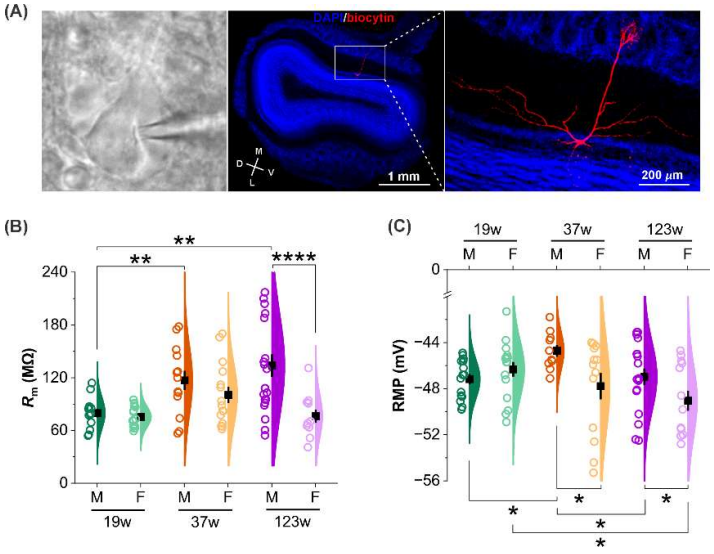

Figure 2. Sex-dependent age influence on membrane properties. (**A**) Left panel: IR-DIC image showing a mitral cell targeted for whole-cell patch-clamp recording. Middle panel: confocal image of a coronal OB section treated with streptavidin-CY3 (red) to bind biocytin in the recorded MC and counterstained with DAPI (blue). Right panel: blown-up from the middle one highlighting the representative morphology of a mitral cells labeled with biocytin (red) via a patch electrode. (**B**) Comparison of mitral cells membrane resistance (R_m) among three age groups in males (n = 13 at 19W, n = 13 at 37W, n = 21 at 123W) and females (n= 17 at 19W, n= 15 at 37W, n= 11 at 123W). (**C**) Resting membrane potential (RMP) in mitral cells across age groups in males (n= 15 at 19W, n= 10 at

 doi:10.20944/preprints202603.0474.v1

37W, n= 18 at 123W) and females (n= 16 at 19W, n= 13 at 37W, n= 13 at 123W). Each data point represents a single cell. Black symbols represent Mean ± SEM. Two-Way ANOVA test, Holm-Bonferroni correction, *p< 0.05, **p< 0.01, ****p< 0.0001.

3.3. Sex-specific age effects on mitral cell action potential characteristics

To characterize how aging influences mitral cell (MC) excitability, we quantified action potential (AP) threshold, amplitude, and afterhyperpolarization (AHP) across three age groups in both sexes using current clamp recordings. We analyzed both spontaneous and evoked action APs (Figure 3A) to capture intrinsic firing properties under resting and depolarizing conditions, providing a comprehensive assessment of age-related excitability changes.

Since some MCs did not fire spontaneous APs, evaluating thresholds of evoked APs ensured a comprehensive assessment of age-related excitability changes. In male mice, the thresholds for both spontaneous and evoked APs were significantly more hyperpolarized at 19 and 123 weeks compared to 37 weeks (p <0.05; Figure 3B, p <0.01; Figure 3E), suggesting reduced excitability at the mid-ages since more depolarization is required to trigger an action potential. In females, evoked AP thresholds exhibited similar age-dependent differences (p <0.05; p <0.01; Figure 2E).

Evoked AP amplitude in males declined significantly at 123 weeks compared to younger ages (p <0.01; Figure 3F), suggesting diminished spike output in aged males. In females, MCs at 37 weeks consistently exhibited reduced amplitudes in both spontaneous and evoked APs relative to the other two age groups (Figure 3C and F).

AHP amplitude, a key regulator of excitability, showed age-dependent differences only in females. Specifically, cells at 37 weeks exhibited significantly smaller AHPs following both spontaneous and evoked action potentials (Figure 3D and G), suggesting enhanced excitability at this age.

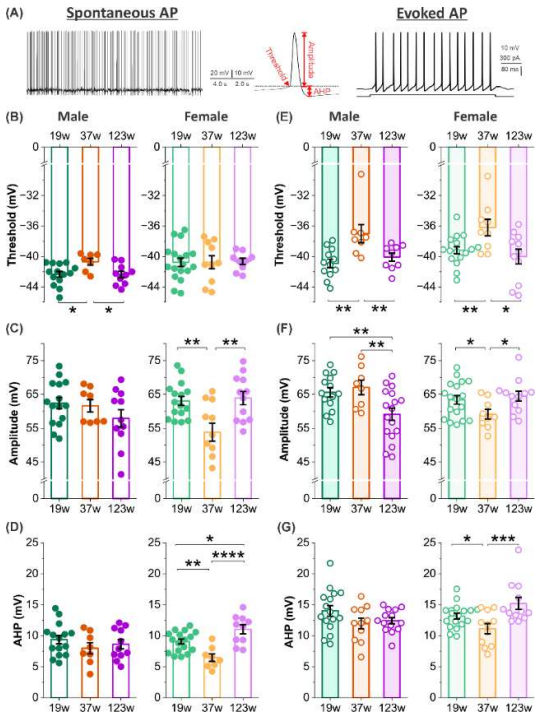

Figure 3. Sex-dependent age effects on action potential characteristics. (A) Left and right panels: representative traces of spontaneous (left) and evoked action potentials recorded under whole-cell current-clamp. Middle panel: a single expanded spike (from left panel) showing the measurement of threshold, amplitude, and afterhyperpolarization (AHP). (B-D) Quantitation of threshold (B, n= 14 at 19W, n= 7 at 37W, n= 10 at 123W in males whereas n= 18 at 19W, n= 10 at 37W, n= 9 at 123W), amplitude (C, n= 15 at 19W, n= 8 at 37W, n= 11 at 123W in males whereas n= 16 at 19W, n= 11 at 37W, n= 12 at 123W in females), and AHP (D, n= 15 at 19W, n= 8 at 37W,

 doi:10.20944/preprints202603.0474.v1

n= 11 at 123W in males whereas n= 18 at 19W, n= 8 at 37W, n= 10 at 123W in females) of spontaneous action potentials in mitral cells. (E-G) Quantitation of threshold (E, n= 12 at 19W, n= 8 at 37W, n= 9 at 123W in males and n= 17 at 19W, n= 9 at 37W, n= 11 at 123W in females), amplitude (F, n= 14 at 19W, n= 8 at 37W, n= 17 at 123W in males whereas n= 18 at 19W, n= 9 at 37W, n= 12 at 123W in female), and AHP (G, n= 16 at 19W, n= 11 at 37W, n= 14 at 123W in males whereas n= 18 at 19W, n= 11 at 37W, n= 12 at 123W in females) of evoked action potentials in mitral cells. Bars show mean ± SEM. Statistical comparisons were performed using One-Way ANOVA followed by Holm-Bonferroni correction. *p< 0.05, **p< 0.01, ***p< 0.001. ****p< 0.001.

3.4. Opposing Age Effects on Spontaneous Firing in Male and Female Mitral Cells with Consistent Trends in Evoked Excitability

MCs in male mice exhibited a clear age-dependent increase in both spontaneous and evoked action potential frequencies. Spontaneous firing at 123 weeks was significantly higher than at 19 and 37 weeks (both p <0.0001) (Figure 4B), coinciding with the highest membrane resistance observed at this age (Figure 2B). This suggest that even small synaptic inputs may be sufficient to depolarize the cell membrane and trigger spontaneous firing in aged males. Similarly, evoked firing frequency at moderate current steps (60–100 pA) was significantly greater in 123-week-old males compared to 37-week-old animals (60 and 100 pA: p <0.01; 80 pA: p <0.05) (Figure 4A and 4D) and resembled the firing rates of the 19-week-old group. These findings indicate heightened excitability of MCs in aged male mice.

In contrast, female mice showed an age-related peak in spontaneous firing frequency at 37 weeks, significantly higher than 19 weeks and 123 weeks (p <0.01; p <0.001; Figure 3C). This pattern is consistent with the elevated membrane resistance (Figure 2B) and reduced AHP amplitude (Figure 3D) in females at this age, which together favor more frequent spontaneous firing due to easier membrane depolarization and shorter interspike intervals.

However, evoked firing frequencies in female MCs did not show a clear age-dependent trend, with significant differences appearing only at select current steps. For instance, MCs from 123-week-old females fired more frequently than those at 37 weeks at 60 pA (p <0.01), 200 pA (p <0.05), or 220 pA (p <0.01), while 19-week-old MCs outpaced 37-week-old MCs at 80 pA, 100 pA, 200 pA or 220 pA (p <0.05) (Figure 4E). Despite these inconsistencies with spontaneous firing data, the evoked spike results align with the more depolarized AP threshold observed at certain ages (Figure 3E).

Collectively, these findings reveal a sex-specific, age-dependent modulation of spontaneous firing in MCs: males show a progressive increase with age, while females peak at mid-age. In contrast, evoked firing patterns show more consistent age effects across sexes, albeit with greater variability in females.

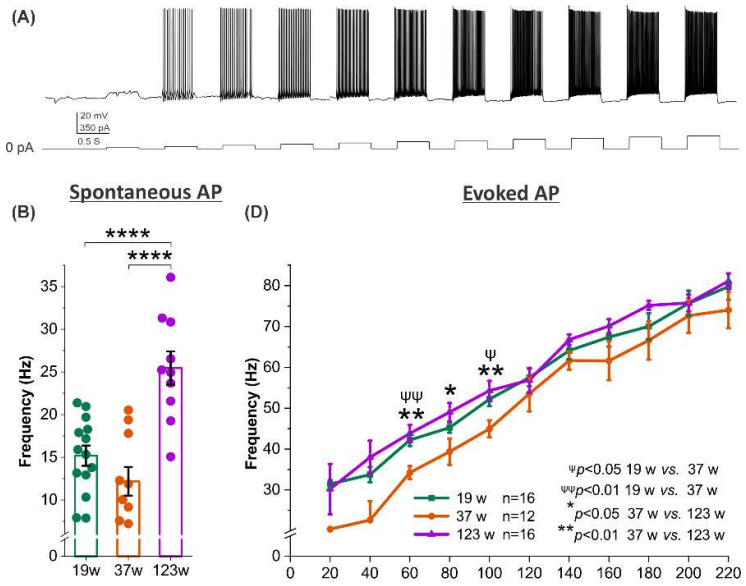

 doi:10.20944/preprints202603.0474.v1

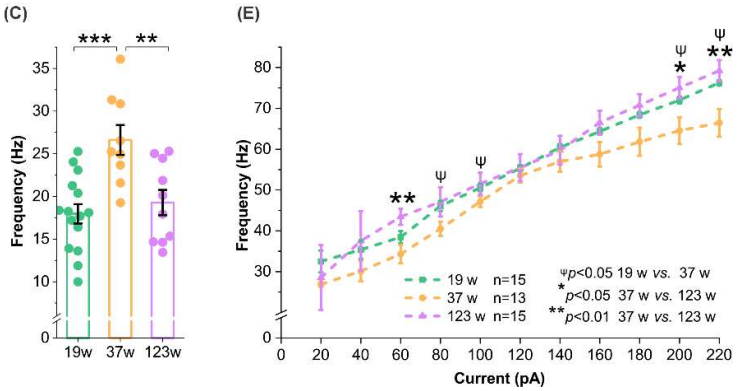

Figure 4. Sex-dependent age impact on firing frequency. (**A**) Representative evoked responses to step current injection recorded in current clamp (top). A series of 500-ms current steps was delivered every 5 s, starting from 0 pA with a 20 pA/step increment (bottom). (**B**) **and** (**C**) Comparison of spontaneous AP firing frequency in MC among three different age groups of males (B, n= 14 at 19W, n= 10 at 37W, n= 10 at 123W) or female (C, n= 15 at 19W, n= 9 at 37W, n= 10 at 123W) mice. Data are presented as mean ± SEM, with each dot representing one cell. ***p*< 0.01, ****p*< 0.001, *****p*< 0.0001. (**D**) **and** (**E**) Input-output relationship showing the frequency of action potentials evoked by increasing current injection in mitral cells of male (D) or female (E) animals. Statistical significance was assessed using One-Way ANOVA followed by Holm-Bonferroni correction.

3.5. Sex effects on threshold, amplitude and afterhyperpolarization of action potentials

It has long been recognized that women outperform men in various olfactory functions including odor detection, identification, and memory across a wide age range (5-99 years)(Doty et al., 1984, Doty and Cameron, 2009), indicating that factors beyond hormone differences contribute to these sex-dependent effects(Doty and Cameron, 2009). To investigate whether functional activity of mitral cells contributes to such differences, we examined sex-specific variations in MC action potential threshold, amplitude, and afterhyperpolarization (AHP). Sex differences in action potential threshold were observed at 19 and 123 weeks of age. At 19 weeks, MCs from female mice showed more depolarized thresholds for both spontaneous and evoked action potentials compared to males (p <0.05) (Figure 5A and D). A similar depolarized threshold was observed in aged females (123 weeks), but only for spontaneous action potentials (Figure 5A). Combined with observed sex differences in membrane resistance in aged mice, these findings suggest that MCs in aged males may be more excitable than those in age-matched females.

Differences in action potential amplitude exhibited a distinct pattern: females had higher amplitudes in evoked spikes at 123 weeks (p <0.05; Figure 5E), but lower amplitudes in both spontaneous and evoked spikes at 37 weeks (p <0.05, p <0.01; Figure 5B and E).

In contrast, sex differences in AHP amplitude were only significant at 123 weeks, where female MCs showed higher AHP amplitudes in both spontaneous and evoked action potentials (p <0.05; Figure 5C).

Taken together, these findings highlight complex, age-dependent interactions between sex and intrinsic membrane properties in MCs, suggesting that overall excitability and output are influenced by a combination of factors that vary across lifespan and sex.

 doi:10.20944/preprints202603.0474.v1

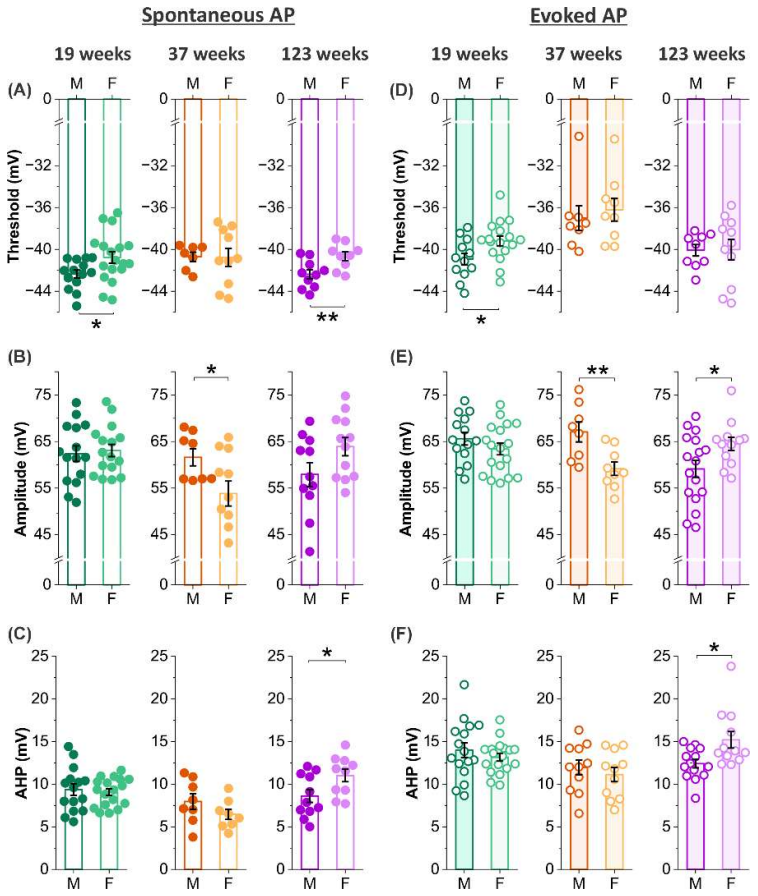

Figure 5. Age-dependent sex influence on action potential characteristics. (**A-C**) Comparison of threshold (A), amplitude (B), and afterhyperpolarization (AHP) amplitude (C) of spontaneous action potentials in mitral cells between male and female mice at the age of 19 weeks (threshold: n=14 cells in male and 18 cells in female; amplitude: n=15 cells in male and 16 cells in female; AHP: n=15 cells in male and 18 cells in female), 37 weeks (threshold: n = 7 cells in male and 10 cells in female; amplitude: n = 8 cells in male and 11 cells in female; AHP: n = 8 cells in male and 8 cells in female), or 123 weeks (threshold: n = 10 cells in male and 9 cells in female; amplitude: n = 11 cells in male and 12 cells in female; AHP: n = 11 cells in male and 10 cells in female). (**D-F**) Comparison of threshold (D), amplitude (E), and afterhyperpolarization (AHP) amplitude (F) of evoked action potentials in mitral cells between male and female mice at the age of 19 weeks (threshold: n = 12 cells in male and 17 cells in female; amplitude: n = 14 cells in male and 18 cells in female; AHP: n = 16 cells in male and 18 cells in female), 37 weeks (threshold: n = 8 cells in male and 9 cells in female; amplitude: n = 8 cells in male and 9 cells in female; AHP: n = 11 cells in male and 11 cells in female), or 123 weeks (threshold: n = 9 cells in male and 11 cells in female; amplitude: n = 17 cells in male and 12 cells in female; AHP: n = 14 cells in male and 12 cells in female). Each solid or open dot represents one recorded cell. Bars with error symbols represent mean ± SEM. Statistical comparisons were performed using Two-Sample t-Test followed by Welch Correction. *$p < 0.05$, **$p < 0.01$.

3.6. Age-dependent sex modulation of spontaneous but not evoked firing

Although no sex difference is observed in either spontaneous or evoked action potential frequencies in MCs of animals at 19 weeks of age (Figure 6A and D), sex- and age-dependent effects emerged in the other two age groups. Specifically, MCs in female mice exhibited a higher spontaneous firing rate than males at 37 weeks ($p < 0.0001$; Figure 6B), but a lower firing rate at 123 weeks ($p < 0.05$; Figure 6C). These differences align with the observed changes in afterhyperpolarization (AHP) amplitude of spontaneous action potentials: females showed a larger AHP at 123 weeks compared to age-matched males (Figure 5C). Since AHP negatively regulates the

 doi:10.20944/preprints202603.0474.v1

frequency of repetitive spiking, these findings support a mechanistic link between AHP dynamics and sex-specific spontaneous firing rates. In contrast, no sex differences were detected in evoked action potential frequencies across all three age groups (Figure 6D-F), potentially due to opposing sex effects on cell membrane properties that neutralize each other during strong stimulation. Collectively, these results implicate that MC responses to weak excitatory input are subject to modulation of sex and age interactions, influencing the system's background activities, whereas their response to strong excitatory input remain sex-independent throughout aging.

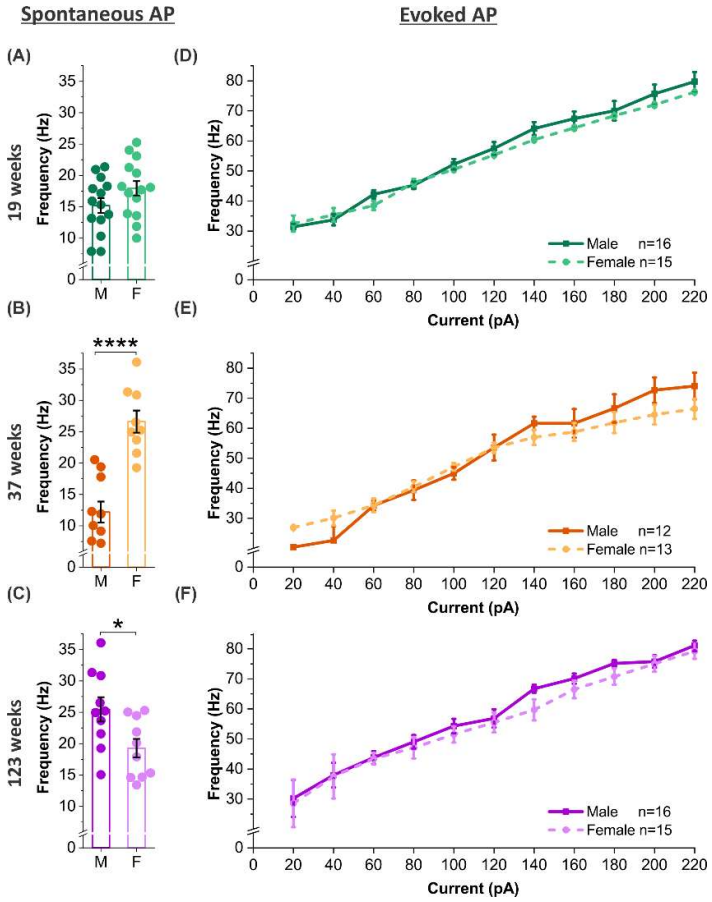

Figure 6. Sex age-dependently impacts spontaneous firing frequency. (**A-C**) Comparison of spontaneous action potential frequency in mitral cells between males and females at the age of 19 weeks (A, n = 14 cells in male and 15 cells in female), 37 weeks (B, n = 10 cells in male and 9 cells in female), and 123 weeks (C, n = 10 cells in male and 10 cells in female). Each dot represents one recorded cell. Bars with error symbols represent mean ± SEM. (**D-F**) Comparison of evoked action potential frequency across increasing step currents at the age of 19 weeks (D), 37 weeks (E), and 123 weeks (F) with sample sizes indicated by the legends of each panel. Statistical comparisons were performed using Two-Sample t-Test followed by Welch Correction. *p< 0.05, ****p< 0.0001.

3.7. Sex-dependent age signatures in synaptic excitation

To evaluate the effect of aging on excitatory synaptic activity, spontaneous excitatory postsynaptic currents (sEPSCs) were recorded and analyzed from MCs across three age groups in both sexes (Figure 7A). In male MCs, the cumulative probability distribution for both amplitude and frequency of sEPSCs shifted leftward from 19 weeks to 37 weeks and 123 weeks, indicating an age-related decline in excitatory synaptic input from the local circuits. Specifically, 19-week-old males exhibited significantly higher sEPSC amplitude and frequency compared to both 37- and 123-week groups (p <0.0001, p <0.001; Figure 7B).

 doi:10.20944/preprints202603.0474.v1

Similar patterned differences were also observed in female MCs. While the cumulative probability distribution of sEPSC frequency was indistinguishable between 19 and 37 weeks, a pronounced leftward shift was seen in the 123-week group compared to the other two age groups (p <0.0001, p <0.01; Figure 7C). Additionally, sEPSC amplitude decreased in the 123-week group compared to the other two younger groups (p <0.0001; Figure 7C), although the cumulative probability curves for 19 and 37 weeks crossed, suggesting more nuanced differences between these two time points.

Overall, these results demonstrate a progressive, age-related decline in excitatory synaptic input to MCs in both sexes, likely reflecting reduced afferent drive or synaptic connectivity. This shared synaptic weakening may underlie deficits in olfactory processing observed with aging.

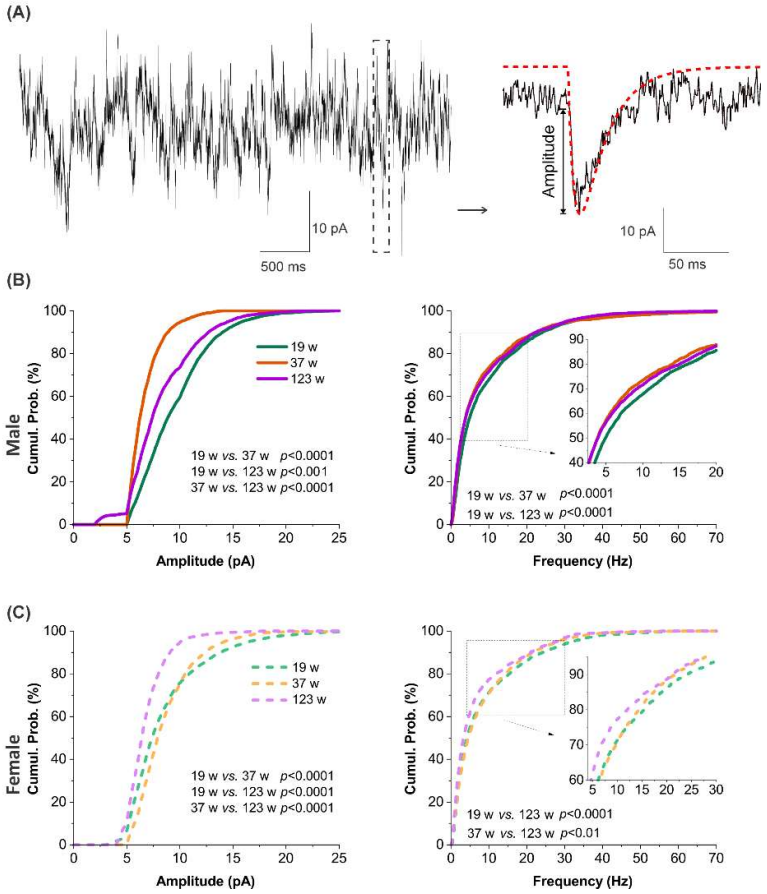

Figure 7. Age-related differences in spontaneous excitatory synaptic transmission. (**A**) Left: representative trace of spontaneous excitatory postsynaptic currents (sEPSCs) recorded from a mitral cell using whole-cell voltage clamp at -60 mV. Right: blown-up of a single sEPSC waveform from the trace on the left, overlaid with detection template (red dotted curve) used for event detection and analysis. (**B and C**) cumulative probability plots comparing sEPSC amplitude (left) or frequency (right) in mitral cells from male (B, n= 17 at 19W, n= 8 at 37W, n= 18 at 123W) or female (C, n= 15 at 19W, n= 13 at 37W, n= 10 at 123W) mice among three age groups. n represents the number of mitral cells recorded in each group. Statistical comparisons were performed using the Mann-Whitney Test (nonparametric).

 doi:10.20944/preprints202603.0474.v1

3.8. Sex-dependent alterations in excitatory synaptic input across ages

Sex differences in spontaneous excitatory synaptic activity exhibited a dynamic, age-dependent trajectory. At 19 weeks, male MCs showed significantly higher sEPSC amplitude and frequency than females (p <0.0001; Figure 8A), suggesting stronger excitatory input in early adulthood. This pattern reversed at 37 weeks, with female MCs exhibiting significantly elevated amplitude (p <0.0001) and frequency (p <0.001) compared to males (Figure 8B). By 123 weeks, the initial trend reemerged, with male MCs again displaying significantly greater sEPSC amplitude and frequency than age-matched females (p <0.0001; Figure 8C). These results reveal a non-monotonic, sex-dependent modulation of excitatory synaptic input, characterized by a transient mid-life enhancement in females followed by a marked decline in advanced age.

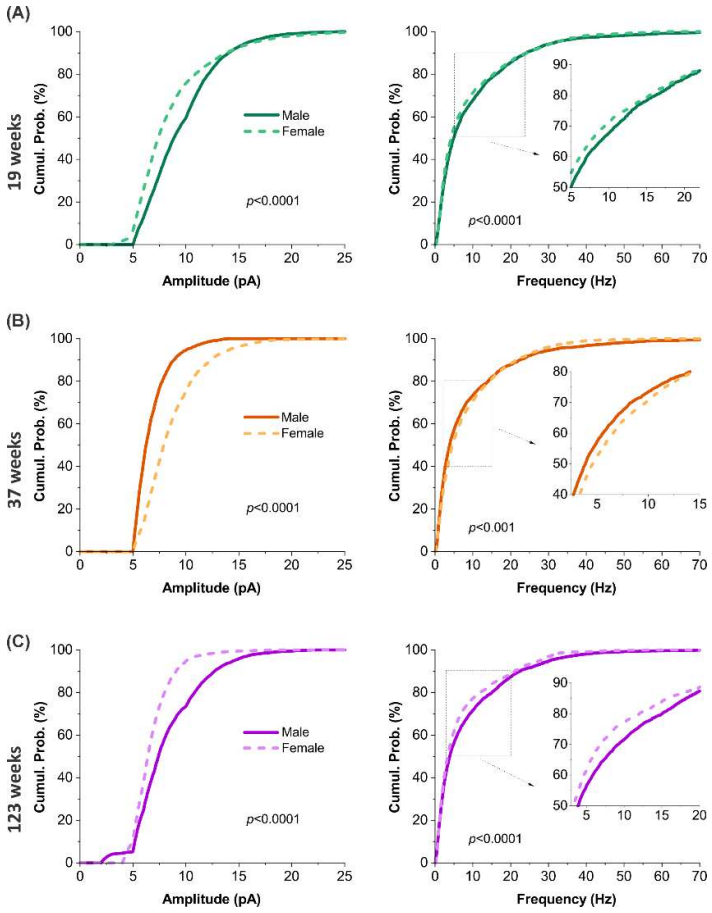

Figure 8. Sex-dependent variations in spontaneous excitatory synaptic activity across aging. (**A-C**) cumulative probability plots comparing sEPSC amplitude (left) and frequency (right) in mitral cells between male (blue) and female (red) mice at three ages: 19 weeks (A, n = 17 cells in male and 15 cells in female), 37 weeks (B, n = 8 cells in male and 13 cells in female), or 123 weeks (C, n = 18 cells in male and 10 cells in female). Statistical analysis and comparison were conducted using the nonparametric Mann-Whitney Test.

4. Discussion

Normal physiological aging is accompanied by progressive alterations in sensory processing and neuronal function(Olofsson et al., 2021). The olfactory system, characterized by well-defined circuitry and sustained functional engagement across the lifespan(Lledo et al., 2006, Doty and Kamath, 2014), provides a particularly accessible framework for examining the cellular foundations of brain aging(Mobley et al., 2014). However, despite substantial progress in characterizing the behavioral and clinical manifestations of age-related olfactory decline, the cellular and physiological

 doi:10.20944/preprints202603.0474.v1

mechanisms that confer late-life vulnerability to central olfactory circuits remain incompletely understood. In particular, how aging interacts with sex to shape neuronal physiology within the primary output neurons of the olfactory bulb has yet to be clearly resolved. To address this knowledge gap, our study provided a comprehensive, age- and sex-stratified characterization of intrinsic and synaptic properties of MCs in mouse OB slices. In parallel, we observed age- and sex-dependent alterations in olfactory-guided foraging behavior, with older animals showing reduced search efficiency and females exhibiting the strongest impairment, indicating that system-level deficits accompany the cellular vulnerabilities identified here. Crucially, our experimental design incorporated not only young and aging animals, but also an advanced-age cohort (123 weeks) nearing the natural lifespan limit of laboratory mice. This set our work apart from others with limitations to brain slices from animals under 100 days old due to technical constraints. More importantly, it enabled us to capture the full continuum of age-related neuronal changes, including those occurring at the very threshold of natural senescence—thus offering rare and critical insights into the physiological basis of late-life brain vulnerability and sensory decline.

Our study is the first to identify, at the single-cell level, a unique pattern of lifespan remodeling in the membrane properties of MCs: in males, R_m increases steadily with age, peaking in advanced age, while in females, R_m reaches its maximum at midlife and subsequently declines. This non-monotonic, sex-divergent trajectory was not observed in previous patch-clamp studies, which typically analyzed only a single sex or pooled both sexes without stratified comparison, thereby missing finer age- and sex-dependent remodeling patterns(Gadiwalla et al., 2025, Kolling et al., 2025, Ackels et al., 2020). These results directly complement recent multi-omics research, which demonstrates that sex hormones and X-linked genes modulate neural resilience and aging trajectories at the molecular level(Arnold and Lusis, 2012, Khramtsova et al., 2019). Recent studies have shown that estrogen signaling and sex-chromosome dosage affect neuronal plasticity and vulnerability, particularly in the context of aging and neurodegeneration(Mei et al., 2025, Villa et al., 2016, Brinton et al., 2015, Davis et al., 2020). In addition to R_m, we observed that RMP in MCs also undergoes marked age- and sex-dependent remodeling. Specifically, RMP in males is most depolarized at midlife, whereas in females, it exhibits a progressive hyperpolarization throughout the lifespan. This pattern parallels recent evidence from studies in cortical, locus coeruleus and hippocampal neurons(Barzó et al., Lee et al., 2024, Power et al., 2002, Disterhoft et al., 2004), where age- and sex-dependent alterations in neuronal excitability and baseline membrane properties have been identified, highlighting a common theme of brain region- and sex-specific electrophysiological remodeling during aging. By extending these findings to the OB, our results underscore that both R_m and RMP are modulated through the interplay of age and sex, providing a cellular basis for sex-specific olfactory processing and vulnerability to neurological disease.

Building on these findings, we further analyzed how age and sex interactively shape additional intrinsic properties and firing output of mitral cells across the lifespan. In male mice, both spontaneous and evoked AP firing frequencies increased markedly with age, especially in advanced age (123 weeks). This heightened excitability paralleled an increase in R_m and a hyperpolarized shift in AP threshold, while AHP amplitude remained relatively stable. These patterns align with prior work by Fadool et al.(Fadool et al., 2011), who demonstrated that elevated input resistance and altered potassium channel function contribute to enhanced excitability and reduced AP amplitude in male MCs, likely reflecting underlying metabolic and ion channel remodeling. Notably, persistent increases in MC excitability during advanced age—particularly when accompanied by changes in input resistance and AP threshold—may not indicate functional preservation, but rather a maladaptive regulatory shift. Accumulating evidence suggests that sustained neuronal hyperexcitability is a fundamental and early hallmark of brain aging, often preceding and promoting vulnerability to cognitive decline and neurodegeneration(Park et al., 2025, Gonzales et al., 2022). Such maladaptive compensation could destabilize mitral cell networks and increase susceptibility to excitotoxic stress or synaptic dysfunction, as observed in other brain regions and aging models. Female MCs, by contrast, exhibited a clear midlife (37-week) peak in spontaneous firing frequency,

 doi:10.20944/preprints202603.0474.v1

corresponding with a marked reduction in AHP amplitude and a modest increase in R_m, while AP threshold remained comparatively stable. Pharmacological inhibition of AHP has been shown to increase MC firing rates and shorten interspike intervals(Duménieu et al., 2015), supporting the interpretation that natural midlife AHP reduction underlies heightened excitability in females. However, despite this pronounced modulation of spontaneous activity, evoked firing frequencies in female MCs did not display a consistent age-related trend, differing only at select current steps. This suggests that, in the context of strong depolarizing input, the influence of intrinsic properties such as AHP and membrane resistance on spike output may be diminished, and age- or sex-dependent differences are more apparent under baseline or weak input conditions.

To further extend our investigation beyond intrinsic firing properties, we proceeded to analyze synaptic transmission by recording sEPSCs in MCs, focusing on both frequency and amplitude. Our results revealed a clear trend of progressive decline in excitatory synaptic input with advancing age, observed in both males and females. Previous magnetic resonance imaging studies in male mice revealed that OB volume and layer thickness decrease with aging, alongside declines in odor discrimination ability(Bontempi et al., 2023). The progressive decrease in sEPSC frequency and amplitude observed in our recordings mirrors these anatomical and molecular findings, providing a single-cell electrophysiological perspective on the synaptic remodeling that occurs during aging in the OB. In females, excitatory synaptic input to MCs remained stable from young to midlife and declined sharply only in advanced age, a non-monotonic pattern mirrored by immunohistochemical and electron microscopy quantification evidence showing delayed but more abrupt loss of glutamatergic synapses in the OB(Richard et al., 2010). Multi-omics and clinical studies have further demonstrated that accelerated synaptic and cognitive decline in olfactory and memory circuits is a prominent endophenotype in women with AD, and that this increased vulnerability is closely linked to hormonal regulation (particularly estrogen), molecular signatures of synaptic and inflammatory pathways, and distinct genetic risk factors(Mei et al., 2025, Zhu et al., 2021). In males, the reduction in excitatory synaptic input occurred earlier and progressed more gradually, as evidenced by electrophysiological recordings and by anatomical studies reporting age-related decreases in OB synaptic density and structural volume(Bontempi et al., 2023, Conley et al., 2003, Richard et al., 2010, Ahnaou et al., 2020). Epidemiological and molecular analyses indicate that olfactory dysfunction and neurodegeneration associated with Parkinson's disease tend to appear earlier and with greater prevalence in men, potentially reflecting enhanced susceptibility of olfactory and dopaminergic circuits, as well as the influence of lower estrogen levels in aging males(Cattaneo and Pagonabarraga, 2025, Schaffner et al., 2025). Taken together, our data provide single-cell electrophysiological evidence that aging and sex exert distinct and temporally structured effects on excitatory synaptic input to olfactory bulb mitral cells, revealing sex-specific trajectories of synaptic remodeling across the lifespan that align with broader patterns of brain aging and may confer differential vulnerability in late life.

This study maps age- and sex-dependent functional remodeling in MCs with whole cell patch clamp recordings in OB slices. This enabled detailed analysis of membrane and local synaptic properties. However, the ex vivo approach excluded long-range inputs and neuromodulators like dopamine and acetylcholine, which influence MC excitability and plasticity in vivo(Ahnaou et al., 2020, Brunert and Rothermel, 2021). Artificial CSF also lacks metabolic and hormonal factors relevant to aging and sex, which modulate age-related vulnerability in MCs(Ekanayake et al., 2024, Dan et al., 2023, Russell et al., 2019). As such, our findings may not directly translate to in vivo functional or behavioral outcomes. Future studies incorporating viral tracing, multi-site electrophysiology, and functional imaging will be essential to determine how age- and sex-dependent remodeling of OB mitral cell circuits is integrated across distributed brain networks, and how these interacting factors shape divergent trajectories of circuit function and vulnerability in later life, including contexts relevant to neurodegenerative disease.

 doi:10.20944/preprints202603.0474.v1

5. Conclusion

This study establishes the first comprehensive single-cell electrophysiological evidence that mitral cells in the olfactory bulb undergo distinct, age- and sex-dependent intrinsic and synaptic remodeling across the mouse lifespan. These findings reveal previously unappreciated complexity in sensory circuit vulnerability and demonstrate that aging and biological sex jointly shape the trajectories of olfactory system function in later life. By defining detailed electrophysiological benchmarks for mitral cell remodeling, this work provides a cellular framework for future studies aimed at identifying early markers of circuit aging and sex-specific vulnerability, with potential relevance to sensory and cognitive decline observed in neurodegenerative contexts.

Author Contributions: Conceptualization, S.L. and D.Z.; methodology, D.Z.; behavioral investigation, M.H., D.Z. and C.P.V.; electrophysiological investigation, D.Z.; histology, Y.L.; formal analysis and visualization, D.Z.; writing—original draft preparation, D.Z.; writing—review and editing, D.Z. and S.L.; supervision, S.L. All authors have read and approved the final version of the manuscript.

Funding: This work was supported by the National Institutes of Heal [grant numbers R01AG069196, R01AG074216 and R01AG077541].

Institutional Review Board Statement: All experimental procedures adhered to the National Institutes of Health (NIH) guidelines for the care and use of laboratory animals and were approved by the Institutional Animal Care and Use Committee of the University of Georgia (IACUC).

Conflict of interest statement: The authors declare no competing financial interests.

Acknowledgments: The imaging data used in this publication was produced in collaboration with the Biomedical Microscopy Core at the University of Georgia. This work was supported by the National Institutes of Heal [grant numbers R01AG069196, R01AG074216 and R01AG077541].

References

1. ACKELS, T., JORDAN, R., SCHAEFER, A. T. & FUKUNAGA, I. 2020. Respiration-locking of olfactory receptor and projection neurons in the mouse olfactory bulb and its modulation by brain state. *Frontiers in cellular neuroscience,* 14**,** 220.
2. AHNAOU, A., RODRIGUEZ-MANRIQUE, D., EMBRECHTS, S., BIERMANS, R., MANYAKOV, N., YOUSSEF, S. & DRINKENBURG, W. 2020. Aging alters olfactory bulb network oscillations and connectivity: relevance for aging-related neurodegeneration studies. *Neural Plasticity,* 2020**,** 1703969.
3. ALOTAIBI, M. M., DE MARCO, M. & VENNERI, A. 2023. Sex differences in olfactory cortex neuronal loss in aging. *Frontiers in human neuroscience,* 17**,** 1130200.
4. ARNOLD, A. P. & LUSIS, A. J. 2012. Understanding the sexome: measuring and reporting sex differences in gene systems. *Endocrinology,* 153**,** 2551-2555.
5. ARRUDA, D., PUBLIO, R. & ROQUE, A. C. 2013. The periglomerular cell of the olfactory bulb and its role in controlling mitral cell spiking: a computational model. *PLoS One,* 8**,** e56148.
6. ATTEMS, J., WALKER, L. & JELLINGER, K. A. 2015. Olfaction and aging: a mini-review. *Gerontology,* 61**,** 485-490.
7. BARZÓ, P., SZOTS, I., TÓTH, M., CSAJBÓK, É., MOLNÁR, G. & TAMÁS, G. Electrophysiology and morphology of human cortical supragranular pyramidal cells in a wide age range. bioRxiv. *Preprint] doi,* 10**,** 13.598792.
8. BEAM, C. R., KANESHIRO, C., JANG, J. Y., REYNOLDS, C. A., PEDERSEN, N. L. & GATZ, M. 2018. Differences between women and men in incidence rates of dementia and Alzheimer's disease. *Journal of Alzheimer's disease,* 64**,** 1077-1083.
9. BOESVELDT, S., POSTMA, E. M., BOAK, D., WELGE-LUESSEN, A., SCHÖPF, V., MAINLAND, J. D., MARTENS, J., NGAI, J. & DUFFY, V. B. 2017. Anosmia—a clinical review. *Chemical senses,* 42**,** 513-523.

 doi:10.20944/preprints202603.0474.v1

10. BONTEMPI, P., RICATTI, M. J., SANDRI, M., NICOLATO, E., MUCIGNAT-CARETTA, C. & ZANCANARO, C. 2023. Age-related in vivo structural changes in the male mouse olfactory bulb and their correlation with olfactory-driven behavior. *Biology,* 12**,** 381.
11. BRINTON, R. D., YAO, J., YIN, F., MACK, W. J. & CADENAS, E. 2015. Perimenopause as a neurological transition state. *Nature reviews endocrinology,* 11**,** 393-405.
12. BRUNERT, D. & ROTHERMEL, M. 2021. Extrinsic neuromodulation in the rodent olfactory bulb. *Cell and Tissue Research,* 383**,** 507-524.
13. CATTANEO, C. & PAGONABARRAGA, J. 2025. Sex differences in Parkinson's disease: a narrative review. *Neurology and Therapy,* 14**,** 57-70.
14. CONLEY, D. B., ROBINSON, A. M., SHINNERS, M. J. & KERN, R. C. 2003. Age-related olfactory dysfunction: cellular and molecular characterization in the rat. *American journal of rhinology,* 17**,** 169-175.
15. CROY, I., NORDIN, S. & HUMMEL, T. 2014. Olfactory Disorders and Quality of Life—An Updated Review. *Chemical Senses,* 39**,** 185-194.
16. DAN, X., YANG, B., MCDEVITT, R. A., GRAY, S., CHU, X., CLAYBOURNE, Q., FIGUEROA, D. M., ZHANG, Y., CROTEAU, D. L. & BOHR, V. A. 2023. Loss of smelling is an early marker of aging and is associated with inflammation and DNA damage in C57BL/6J mice. *Aging Cell,* 22**,** e13793.
17. DAVIS, E. J., BROESTL, L., ABDULAI-SAIKU, S., WORDEN, K., BONHAM, L. W., MIÑONES-MOYANO, E., MORENO, A. J., WANG, D., CHANG, K. & WILLIAMS, G. 2020. A second X chromosome contributes to resilience in a mouse model of Alzheimer's disease. *Science translational medicine,* 12**,** eaaz5677.
18. DEACON, R., KOROS, E., BORNEMANN, K. & RAWLINS, J. 2009. Aged Tg2576 mice are impaired on social memory and open field habituation tests. *Behavioural brain research,* 197**,** 466-468.
19. DEJOU, J., MANDAIRON, N. & DIDIER, A. 2024. Olfactory neurogenesis plays different parts at successive stages of life, implications for mental health. *Frontiers in Neural Circuits,* 18**,** 1467203.
20. DÍAZ-GUERRA, E., PIGNATELLI, J., NIETO-ESTÉVEZ, V. & VICARIO-ABEJÓN, C. 2013. Transcriptional regulation of olfactory bulb neurogenesis. *The Anatomical Record,* 296**,** 1364-1382.
21. DISTERHOFT, J. F., WU, W. W. & OHNO, M. 2004. Biophysical alterations of hippocampal pyramidal neurons in learning, ageing and Alzheimer's disease. *Ageing research reviews,* 3**,** 383-406.
22. DOTY, R. L. & CAMERON, E. L. 2009. Sex differences and reproductive hormone influences on human odor perception. *Physiol Behav,* 97**,** 213-28.
23. DOTY, R. L. & KAMATH, V. 2014. The influences of age on olfaction: a review. *Frontiers in psychology,* 5**,** 20.
24. DOTY, R. L., SHAMAN, P., APPLEBAUM, S. L., GIBERSON, R., SIKSORSKI, L. & ROSENBERG, L. 1984. Smell identification ability: changes with age. *Science,* 226**,** 1441-3.
25. DUMÉNIEU, M., FOURCAUD-TROCMÉ, N., GARCIA, S. & KUCZEWSKI, N. 2015. Afterhyperpolarization (AHP) regulates the frequency and timing of action potentials in the mitral cells of the olfactory bulb: role of olfactory experience. *Physiological reports,* 3**,** e12344.
26. EKANAYAKE, A., PEIRIS, S., AHMED, B., KANEKAR, S., GROVE, C., KALRA, D., ESLINGER, P., YANG, Q. & KARUNANAYAKA, P. 2024. A review of the role of estrogens in olfaction, sleep and glymphatic functionality in relation to sex disparity in Alzheimer's disease. *American Journal of Alzheimer's Disease & Other Dementias®,* 39**,** 15333175241272025.
27. FADOOL, D. A., TUCKER, K. & PEDARZANI, P. 2011. Mitral cells of the olfactory bulb perform metabolic sensing and are disrupted by obesity at the level of the Kv1. 3 ion channel. *PloS one,* 6**,** e24921.
28. FLURKEY, K., CURRER, J., HARRISON, D. & FOX, J. G. 2007. The mouse in biomedical research. *American College of Laboratory Animal Medicine series. Elsevier, AP: Amsterdam***,** 637-672.
29. GADIWALLA, S., GUILLAUME, C., HUANG, L., WHITE, S. J. B., BASHA, N., PETERSEN, P. H. & GALLIANO, E. 2025. Ex Vivo Functional Characterization of Mouse Olfactory Bulb Projection Neurons Reveals a Heterogeneous Continuum. *eNeuro,* 12.
30. GONZALES, M. M., GARBARINO, V. R., POLLET, E., PALAVICINI, J. P., KELLOGG, D. L., KRAIG, E. & ORR, M. E. 2022. Biological aging processes underlying cognitive decline and neurodegenerative disease. *The Journal of clinical investigation,* 132.
31. HIRATA, T. 2024. Olfactory information processing viewed through mitral and tufted cell-specific channels. *Frontiers in Neural Circuits,* 18**,** 1382626.

 doi:10.20944/preprints202603.0474.v1

32. KENSAKU, M. 2014. The Olfactory System: From Odor Molecules to Motivational Behaviors. Tokyo: Springer.
33. KHRAMTSOVA, E. A., DAVIS, L. K. & STRANGER, B. E. 2019. The role of sex in the genomics of human complex traits. *Nature Reviews Genetics,* 20**,** 173-190.
34. KOLLING, L. J., MARCINKIEWCZ, C. A. & FADOOL, D. A. 2025. The superficial tufted and mitral cell output neurons of the mouse olfactory bulb have a dual role in insulin sensing. *bioRxiv***,** 2025.04. 15.648999.
35. KONDO, K., KIKUTA, S., UEHA, R., SUZUKAWA, K. & YAMASOBA, T. 2020. Age-related olfactory dysfunction: epidemiology, pathophysiology, and clinical management. *Frontiers in aging neuroscience,* 12**,** 208.
36. LEE, J., WANG, Z. M., MESSI, M. L., MILLIGAN, C., FURDUI, C. M. & DELBONO, O. 2024. Sex differences in single neuron function and proteomics profiles examined by patch-clamp and mass spectrometry in the locus coeruleus of the adult mouse. *Acta Physiologica,* 240**,** e14123.
37. LLEDO, P.-M., ALONSO, M. & GRUBB, M. S. 2006. Adult neurogenesis and functional plasticity in neuronal circuits. *Nature Reviews Neuroscience,* 7**,** 179-193.
38. MACHADO, C. F., REIS-SILVA, T. M., LYRA, C. S., FELICIO, L. F. & MALNIC, B. 2018. Buried Food-seeking Test for the Assessment of Olfactory Detection in Mice. *Bio Protoc,* 8**,** e2897.
39. MEI, Z., LIU, J., BENNETT, D. A., SEYFRIED, N., WINGO, A. P. & WINGO, T. S. 2025. Unraveling sex differences in Alzheimer's disease and related endophenotypes with brain proteomes. *Alzheimer's & Dementia,* 21**,** e70206.
40. MOBLEY, A. S., RODRIGUEZ-GIL, D. J., IMAMURA, F. & GREER, C. A. 2014. Aging in the olfactory system. *Trends in neurosciences,* 37**,** 77-84.
41. MORI, K. & SAKANO, H. 2021. Olfactory circuitry and behavioral decisions. *Annual review of physiology,* 83**,** 231-256.
42. NAGAYAMA, S., HOMMA, R. & IMAMURA, F. 2014. Neuronal organization of olfactory bulb circuits. *Frontiers in neural circuits,* 8**,** 98.
43. OLOFSSON, J. K., EKSTRÖM, I., LARSSON, M. & NORDIN, S. 2020. Olfaction and Aging: A Review of the Current State of Research and Future Directions. *PsyArXiv. November,* 2.
44. OLOFSSON, J. K., EKSTRÖM, I., LARSSON, M. & NORDIN, S. 2021. Olfaction and aging: A review of the current state of research and future directions. *i-Perception,* 12**,** 20416695211020331.
45. PARK, J., HO, R. L., WANG, W.-E., CHIU, S. Y., SHIN, Y. S. & COOMBES, S. A. 2025. Age-related changes in neural oscillations vary as a function of brain region and frequency band. *Frontiers in Aging Neuroscience,* 17**,** 1488811.
46. POWER, J. M., WU, W. W., SAMETSKY, E., OH, M. M. & DISTERHOFT, J. F. 2002. Age-related enhancement of the slow outward calcium-activated potassium current in hippocampal CA1 pyramidal neurons in vitro. *Journal of Neuroscience,* 22**,** 7234-7243.
47. RICHARD, M. B., TAYLOR, S. R. & GREER, C. A. 2010. Age-induced disruption of selective olfactory bulb synaptic circuits. *Proceedings of the National Academy of Sciences,* 107**,** 15613-15618.
48. ROSENTHAL, M., VARELA, M., GARCIA, A. & BRITTON, D. 1989. Age-related changes in the motor response to environmental novelty in the rat. *Experimental gerontology,* 24**,** 149-157.
49. RUSSELL, J. K., JONES, C. K. & NEWHOUSE, P. A. 2019. The role of estrogen in brain and cognitive aging. *Neurotherapeutics,* 16**,** 649-665.
50. SCHAFFNER, S. L., TOSEFSKY, K. N., INSKTER, A. M., APPEL-CRESSWELL, S. & SCHULZE-HENTRICH, J. M. 2025. Sex and gender differences in the molecular etiology of Parkinson's disease: considerations for study design and data analysis. *Biology of Sex Differences,* 16**,** 7.
51. SEIBENHENER, M. L. & WOOTEN, M. C. 2015. Use of the open field maze to measure locomotor and anxiety-like behavior in mice. *Journal of visualized experiments: JoVE***,** 52434.
52. SMITH, S. & HOPP, S. C. 2023. The 5XFAD mouse model of Alzheimer's disease displays age-dependent deficits in habituation to a novel environment. *Aging Brain,* 3**,** 100078.
53. SOROKOWSKI, P., KARWOWSKI, M., MISIAK, M., MARCZAK, M. K., DZIEKAN, M., HUMMEL, T. & SOROKOWSKA, A. 2019. Sex differences in human olfaction: a meta-analysis. *Frontiers in psychology,* 10**,** 242.

 doi:10.20944/preprints202603.0474.v1

54. STARR, E., BUDHATHOKI, R., GILHOOLY, D., CASTILLO, L., HU, M., ZHAO, D., LI, Y. & LIU, S. 2025. CCKergic Tufted Cells Regulate Odor Sensitivity by Controlling Mitral Cell Output in the Mouse Olfactory Bulb. *Journal of Neuroscience,* 45.
55. TZENG, W.-Y., FIGARELLA, K. & GARASCHUK, O. 2021. Olfactory impairment in men and mice related to aging and amyloid-induced pathology. *Pflügers Archiv-European Journal of Physiology,* 473**,** 805-821.
56. VILLA, A., VEGETO, E., POLETTI, A. & MAGGI, A. 2016. Estrogens, neuroinflammation, and neurodegeneration. *Endocrine reviews,* 37**,** 372-402.
57. VINOGRAD, A., TASAKA, G.-I., KREINES, L., WEISS, Y. & MIZRAHI, A. 2019. The pre-synaptic landscape of mitral/tufted cells of the main olfactory bulb. *Frontiers in Neuroanatomy,* 13**,** 58.
58. XU, L., LIU, J., WROBLEWSKI, K. E., MCCLINTOCK, M. K. & PINTO, J. M. 2020. Odor sensitivity versus odor identification in older US adults: associations with cognition, age, gender, and race. *Chemical Senses,* 45**,** 321-330.
59. YAMAGUCHI, M. 2014. Interneurons in the Olfactory Bulb: Roles in the Plasticity of Olfactory Information Processing. *In:* MORI, K. (ed.) *The Olfactory System: From Odor Molecules to Motivational Behaviors.* Tokyo: Springer Japan.
60. YANAI, S. & ENDO, S. 2021. Functional aging in male C57BL/6J mice across the life-span: a systematic behavioral analysis of motor, emotional, and memory function to define an aging phenotype. *Frontiers in aging neuroscience,* 13**,** 697621.
61. YANG, J. & PINTO, J. M. 2016. The epidemiology of olfactory disorders. *Current otorhinolaryngology reports,* 4**,** 130-141.
62. ZHU, D., MONTAGNE, A. & ZHAO, Z. 2021. Alzheimer's pathogenic mechanisms and underlying sex difference. *Cellular and Molecular Life Sciences,* 78**,** 4907-4920.